Int J Adv Manuf Technol (2017) 88:2537–2546
DOI 10.1007/s00170-016-8797-8

ORIGINAL ARTICLE

The hourglass-like heat source model and its application for laser beam welding of 6 mm thickness 1060 steel

Xiaohong Zhan[1] · **Gaoyang Mi**[1,2] · **Qi Zhang**[1] · **Yanhong Wei**[1] · **Wenmin Ou**[1]

Received: 26 October 2015 / Accepted: 18 April 2016 / Published online: 3 June 2016

Abstract An hourglass-like heat source model is developed to simulate the geometry of weld beads of laser beam welding. The welding experiments with different welding parameters were carried out to find whether the welds are full-penetrated or not. The laser powers ranged between 1.0 and 5.0 kW with steps of 1.0 kW. Five levels of the welding speed were used: 1.0, 2.0, 3.0, 4.0, and 5.0 m/min. The numerical analysis based on finite element method was used to predict the shape of weld pools during welding. To give a better representation of weld bead, an hourglass-like heat source model is developed to describe the unique shape of 1060 steel weld bead for laser beam welding without filler metal instead of the commonly used conical heat source. Comparing the predicted fusion profile with the experimental cross section of weld, it is found that hourglass-like heat source model is more consistent with the experimental results than the conical heat source for 1060 steel. In addition, the best heat source parameters are obtained by an error analysis. Compared to the experimental results, the simulated results for the welds using Power = 4000 W and Speed = 2.0 m/s and 5000 W and 2.0 m/s match the experimental results well.

Keywords Laser beam welding · Hourglass-like heat source · Full-penetrated

✉ Gaoyang Mi
nanhangmigaoyang@163.com

[1] Nanjing University of Aeronautics & Astronautics, Nanjing 211100, China

[2] Huazhong University of Science and Technology, Wuhan 430074, China

1 Introduction

Laser beam welding has been widely used in industry engineering with a concentrated heat input [1, 2]. The prominent features of laser beam welding are the low heat input which leads to a small welding distortion and the high welding speed which leads to highly efficiency [3, 4]. The penetration depth of work pieces is a very critical parameter in laser beam welding [5]. The welded work pieces which are not fully penetrated should not be used under normal circumstances. Finite element simulation is proven to be a useful approach to predict the weld bead geometry. During simulation, there are many factors that affect the shape of simulated weld pool in which the heat source model is commonly thought to be the most important one. According to the comparison between experimental and simulated results, the heat source parameters can be optimized before welding which will give a more accurate representation for the welding pool.

The temperature fields for welding process would be accurate only if an accurate heat source model is adopted in the simulation. In addition, the penetration status is directly determined by temperature fields during welding [6]. Thus, many researchers study the modeling approach for heat source parameters during laser beam welding. Du et al. [7] used a heat source model compromising a Gaussian plane heat source to the top surface and a cylindrical heat source along the z-direction to simulate the geometry profile of weld pools during laser beam welding for titanium alloys. The combined heat source they used can reflect the deep penetration of laser beam welding, but the cylinder heat source cannot accurately predict the reducing of the molten width along the z-direction of a laser beam welding bead. Thus, the conical heat source model is proposed to simulate the shape of the molten pool with different beam energy levels during laser beam welding for AISI 304 stainless steel [8]. Compared with the cylinder heat

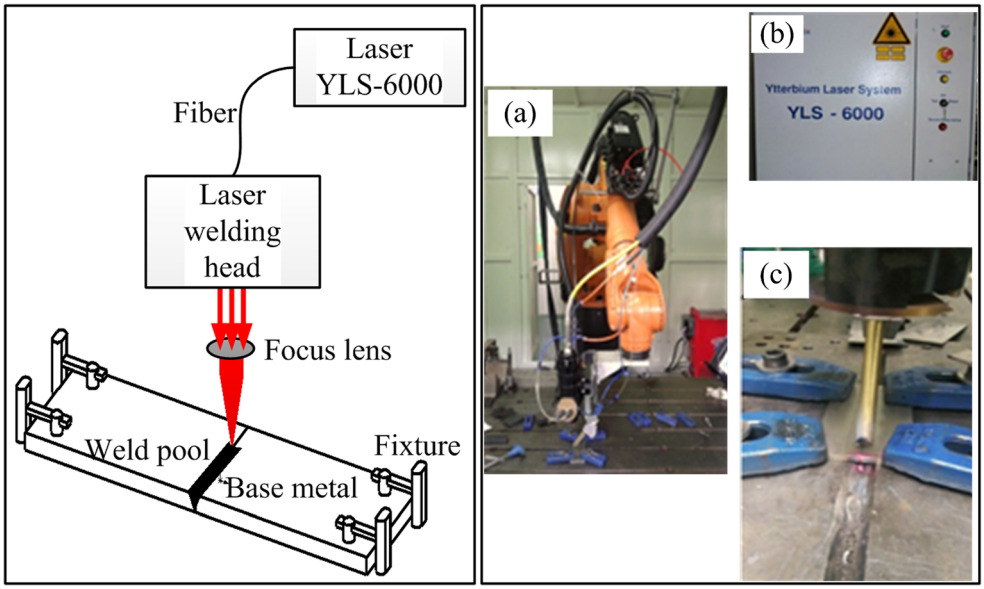

Fig. 1 The sketch and picture of laser welding equipment (**a** KUKA welding robot, **b** YLS-6000 laser source, **c** welding head)

source, the conical heat source model can better reflect the shape of cross section after laser beam welding, especially for the partial penetration weld bead. Lankalapalli et al. [5] developed a two-dimensional finite element (FE) model to estimate penetration depth of laser welding processes. According to the model, the penetration depth is related to the heat input and the Peclet number. They also claimed that since high aspect ratios (about 5–10) can be achieved, which make the heat conduction in the z-direction quite small, so the actual penetration depth is equal to the heat source depth. This work expressed that the weld bead geometry is directly determined by the heat source model during laser beam welding. Therefore, since the geometry parameters of weld bead are influenced by the laser power and welding speed [9], the heat source parameters also should have such relations with the welding parameters. This view point also can be confirmed by the research works published by Sudnik et al. [10]. Dal [11], Hozoorbakhsh [12], Navas [13], and Turner [14] also studied the heat source model for laser welding. It can be seen that two types of weld bead, "nail" type weld bead and the "hourglass" type weld bead, can be achieved by laser beam welding for carbon steel with different thickness [15]. Thus, a new heat source model which is used to represent the hourglass-like weld beads should be proposed to make up for deficiencies of conical heat source model.

In this work, an hourglass-like heat source model is developed to predict the geometry dimensions of weld pool during laser beam welding. The laser beam welding experiments with different laser power and welding speed are carried out to study the relationship between welding parameters and weld bead geometry dimensions. The full-penetrated welds are compared to the simulated weld pools with different welding heat source parameters. An error analysis is carried out to obtain the best heat source parameters.

Table 1 The weld penetrations and weld widths for different weld parameters

	$P=5000$ w	$P=4000$ w	$P=3000$ w	$P=2000$ w	$P=1000$ w	
$S=5$ m/s	3.9	3.4	2.4	1.6	1.0	D
	2.5	2.0	1.5	1.6	1.4	W
$S=4$ m/s	4.6	4.2	3.4	2.6	2.0	D
	3.5	2.5	2.0	1.6	1.4	W
$S=3$ m/s	6.0	5.8	5.0	3.7	3.0	D
	3.5	2.5	2.0	1.7	1.4	W
$S=2$ m/s	6.0	6.0	5.0	4.5	4.5	D
	4.0	2.6	2.3	1.9	1.4	W
$S=1$ m/s	6.0	6.0	6.0	5.5	4.5	D
	4.2	3.4	2.6	2.1	1.8	W

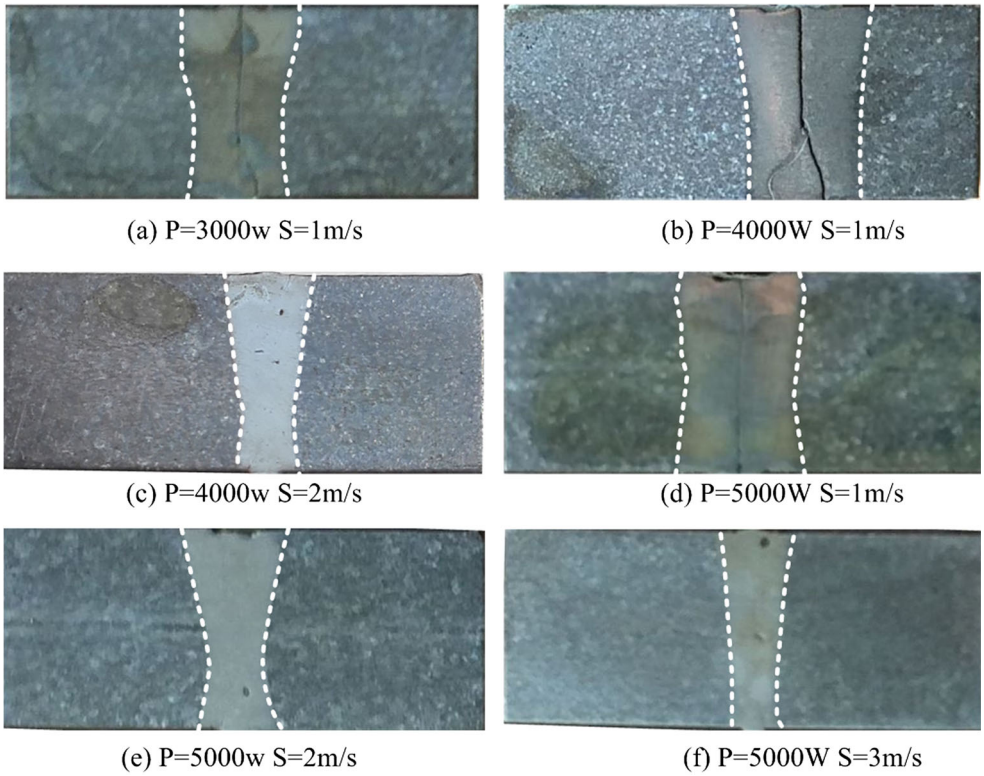

Fig. 2 The experimental cross section of welds for different weld parameters

2 Experiments

The dimensions of work pieces are 100 mm × 50 mm × 6 mm (length × width × thickness). The laser beam welding experiments were carried out in a YLS-6000 laser source. The laser head was moved by using a Kuka (kr30h) welding robot. The sketch and picture of laser welding equipment are shown in Fig. 1.

To investigate the effect of the welding parameters on the weld bead geometry, the components were welded at various values of welding speeds and laser powers. The laser powers ranged between 1.0 and 5.0 kW with steps of 1.0 kW. Five levels of the welding speed were investigated: 1.0, 2.0, 3.0, 4.0, and 5.0 m/min. Since the welding parameters are set in a very large range, unsurprisingly, some of the welds are partial penetration. These results are also valuable if someone would like to study partial penetrated laser beam welding. In this paper, the welds without full-penetrated are ignored.

Metallographic samples were prepared by wire-electrode cutting, grinding by using standard mechanical polishing procedures. Then, the samples were etched in a HNO_3 to C_2H_5OH solution with a volume ratio of 4:96 to show the shape of welds. The weld width and the penetration depth are measured to find whether full penetration is obtained. A set of FE simulations were carried out to determine the heat source parameters which are used to simulate the full penetration laser beam welding for 6 mm thickness 1060 steel.

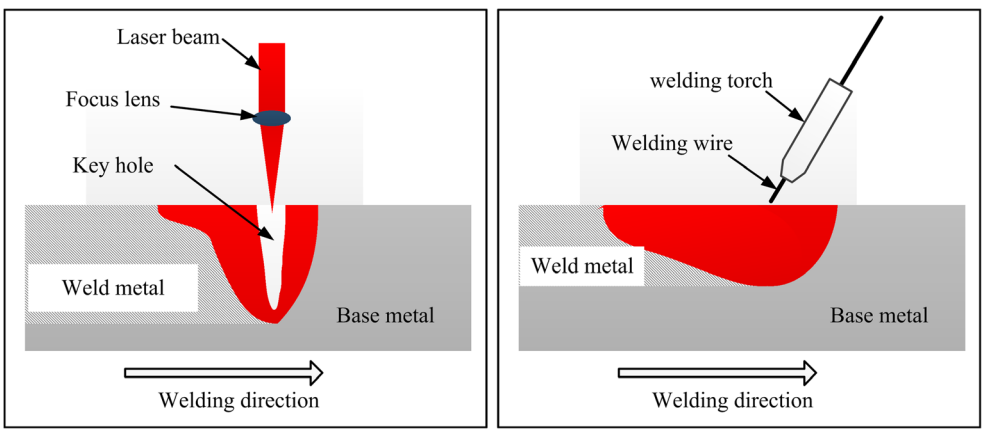

Fig. 3 The schematic diagrams of laser welding and GMAW

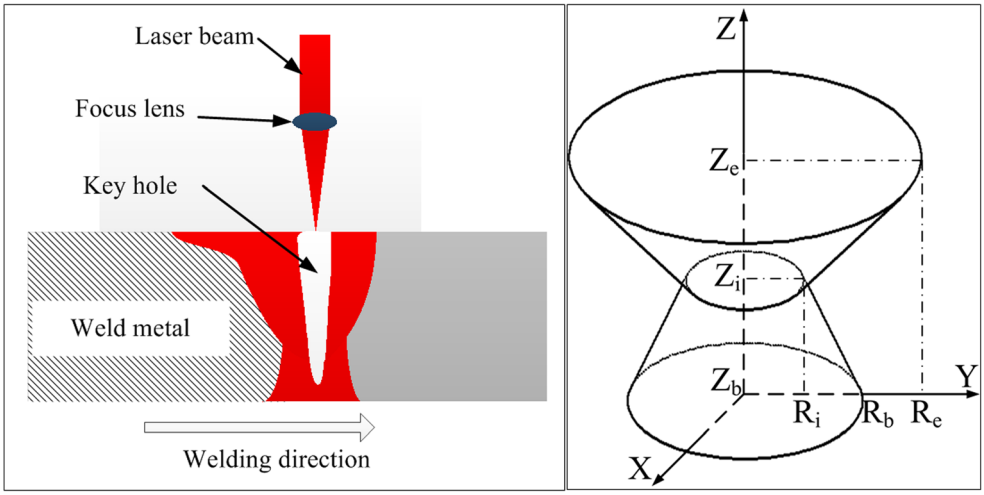

Fig. 4 The schematic diagram of laser welding (*left*) and the hourglass-like heat source model (*right*)

The weld penetration and weld width for different welding parameter groups (combination of laser power and weld speed) are shown in Table 1. In the table, P represents laser power, S represents the welding speed, D represents the weld penetration depth, and W represents the weld width on the top surface of components. The welds which are full-penetrated are highlighted in red.

The cross sections of these welds are presented in Fig. 2.

According to Fig. 2, type "I" crack [16] occurs at the centerline of welds when speed equals to 1 m/min, which is intolerable for the weld components. There are two factors that may cause cracks, the high volume fractions of martensite and too wide weld width. The former is the inevitable result during laser beam welding for a high carbon steel whereas the latter is affected by the relatively slow weld speed for these welds. In theory, the wider welds will decrease the susceptibility of weld cracks since the microstructure is more uniform. However, the laser beam welding experiments in the present work have no filler metal which reduce the feeding ability for the welding pool during cooling. The lack of feeding leads to the formation of cracks at the center line. Since a crack-free weld is usually an important target, the simulations for these three parameter groups are neglected in this work.

Table 2 The constant heat source parameters

Term	z_e	z_b	r_e	r_i	r_b
Value	0.6	0.0	0.6	0.2	0.4

Table 3 The values of changed heat source parameters

Number	η	z_i
1	2/3	0.2
2	2/3	0.3
3	2/3	0.4
4	1/2	0.2
5	1/2	0.3
6	1/2	0.4

3 Numerical models

3.1 Heat source model

A conical heat source model with the Gaussian distribution heat flux is a common choice to simulate the heat input for laser beam welding [17]. The schematic diagram of laser welding and gas metal arc welding (GMAW) are shown in Fig. 3. However, according to the experiments mentioned above, it is seemed that the shape of weld pool of the full-penetrated welds for 1060 carbon steel cannot be accurately characterized by the conical heat source, especially in the bottom of welds. The comparison of fusion profiles between experimental and simulation results based on conical heat source model is mentioned in the previous work [18].

To represent the shape of full penetration welds during laser beam welding for 6 mm thickness 1060 steel, an hourglass-

Table 4 The thermal properties used in the simulation

T	Specific heat (J/g °C)	Thermal conductivity (W/cm °C)
20	0.461	0.418
100	0.496	0.434
300	0.568	0.414
500	0.677	0.367
800	0.778	0.324
1200	0.778	0.313
3000	0.778	0.313

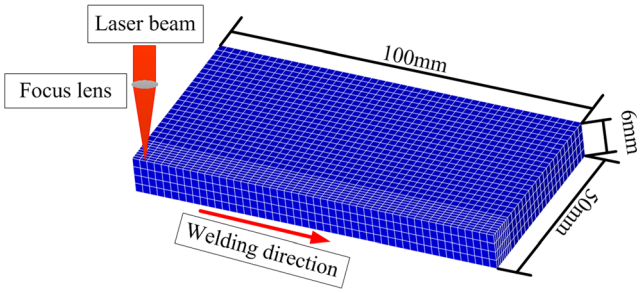

Fig. 5 The mesh used in the simulations

like rotating heat source with Gaussian power density distribution is developed. The schematic diagram of laser welding and the hourglass-like heat source model are shown in Fig. 4, and the heat source looks like two combined frustums.

Where z and r represent the z-axis coordinate and the radium of each surface, the subscript "e", "i," and "b" represent the top surface, middle surface, and bottom surface of the heat source, respectively. After introducing parameters shown in Fig. 4, the heat source model can be expressed as Eq.(1).

$$q_{vT} = \frac{9Q_v}{\pi(1-e^{-3})}\frac{1}{(z_e-z_i)\left(r_e^2+r_e r_i+r_i^3\right)}\exp\left(-\frac{3r^2}{r_c^2}\right) \quad \text{For } z \geq z_i \tag{1a}$$

$$q_{vB} = \frac{9Q_v\eta}{\pi(1-e^{-3})}\frac{1}{(z_i-z_b)\left(r_b^2+r_b r_i+r_i^3\right)}\exp\left(-\frac{3r^2}{r_c^2}\right) \quad \text{For } z < z_i \tag{1b}$$

where

$$r_c = r_i + (r_e - r_i)\left(\frac{z-z_i}{z_e-z_i}\right) \quad \text{For } z \geq z_i.$$

$$r_c = r_i + (r_b - r_i)\left(\frac{z-z_b}{z_i-z_b}\right) \quad \text{For } z < z_i.$$

η is the heat source partition coefficient.

3.2 Heat source parameters

In the present work, z_e, z_b, r_e, r_i, and r_b are constant which are shown in Table 2.

The parameters η and z_i are modified to give a better fit to the experimental results. The values of η and z_i used in the simulation are shown in Table 3.

According to the experimental results, the samples are completely penetrated by using the weld parameters highlighted in red in Table 1. For each group of weld parameters, six

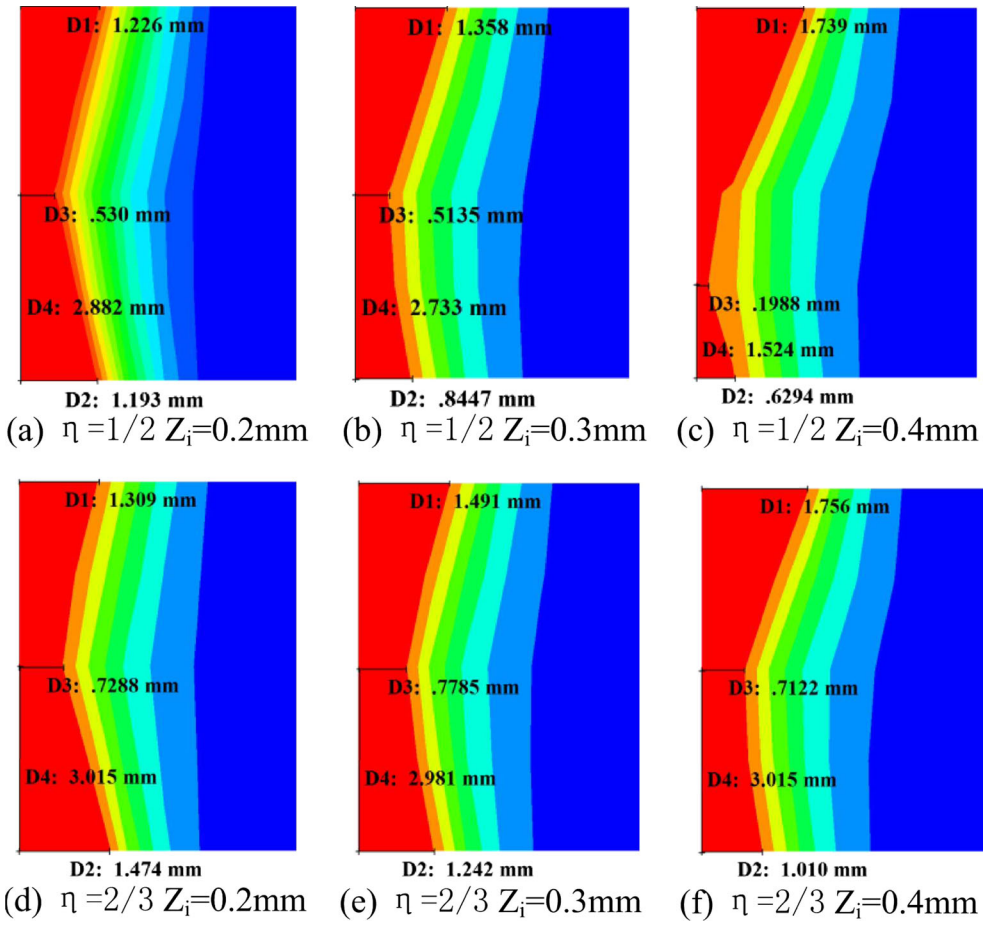

Fig. 6 The simulated cross section of welds (Power = 4000 W, Speed = 2 m/s)

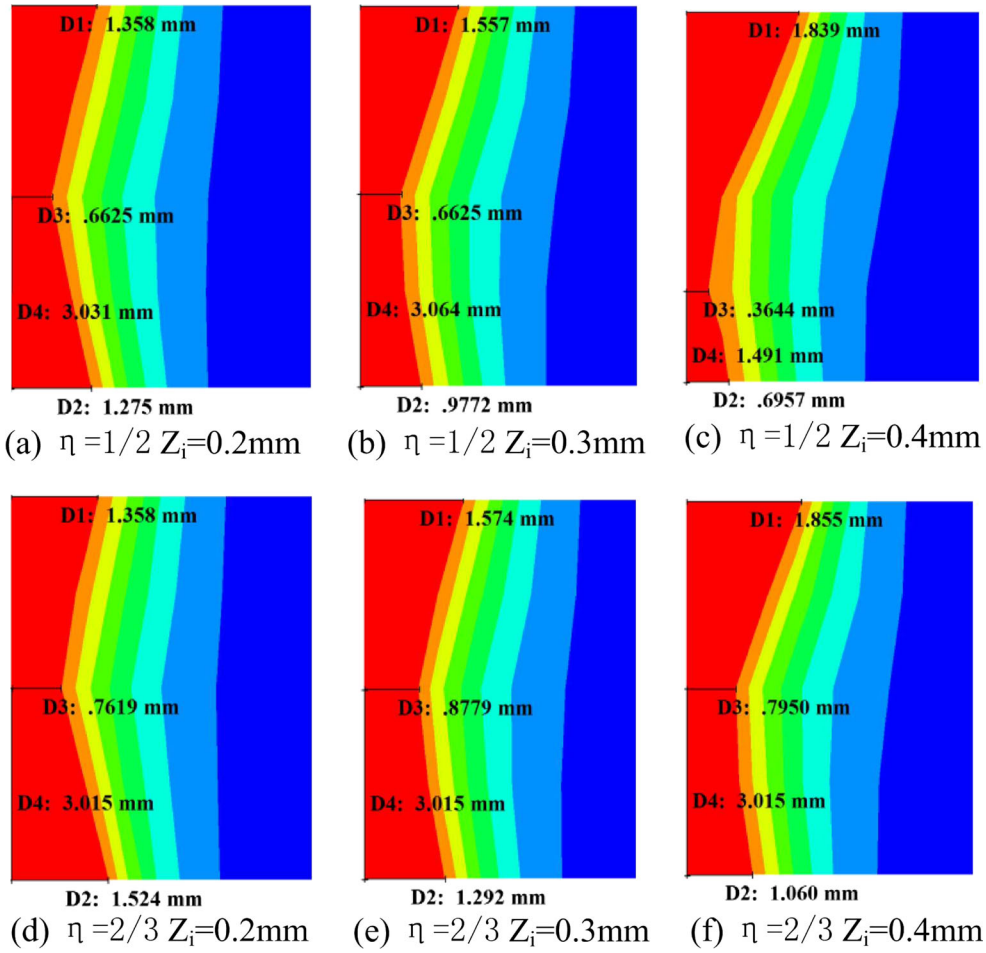

Fig. 7 The simulated cross section of welds (Power = 5000 W, peed = 2 m/s)

simulations with different heat source parameters shown in Tables 2 and 3 are carried out to optimize heat source parameters.

3.3 Thermal properties

The thermal properties used in this work are shown in Table 4. These parameters are exported from a commercial FE software, Simufact.welding.

3.4 Geometry and meshing

The geometry model for simulation is shown in Fig. 5.

4 Results and discussions

According to Fig. 2, the shape of cross section of laser beam welding for 1060 steel is different with the traditional "Nailhead shape" weld. The conical heat source which is the common choice for laser welding is not suitable for this instance. The hourglass-like heat source is proposed to represent such unique shape. Since hourglass-like heat source is a new heat source model, the heat source parameters especially the partition coefficient η and z-axis coordinate of middle surface Z_i need to be determined by using an error analysis.

The simulated cross section of welds based on the heat source parameters shown in Tables 2 and 3 are shown in Figs. 6, 7, and 8.

Four critical distances which are used to represent the shape of welds are named as D1–D4 (See Fig. 9). The experimental and simulated values of D1–D4 are shown in Figs. 10, 11, and 12.

An error analysis is carried out to find the best heat source parameters. The average error is calculated to evaluate the similarity between experimental and simulation results.

$$ERR[Di] = \frac{|[Di](Experimental) - [Di](Simulated)|}{[Di](Experimental)} \quad (2)$$

$$AverERR = \frac{\sum_{1}^{4} ERR[Di]}{4} \quad (3)$$

where $i = 1,2,3,4$ and [Di] represents the four distances.

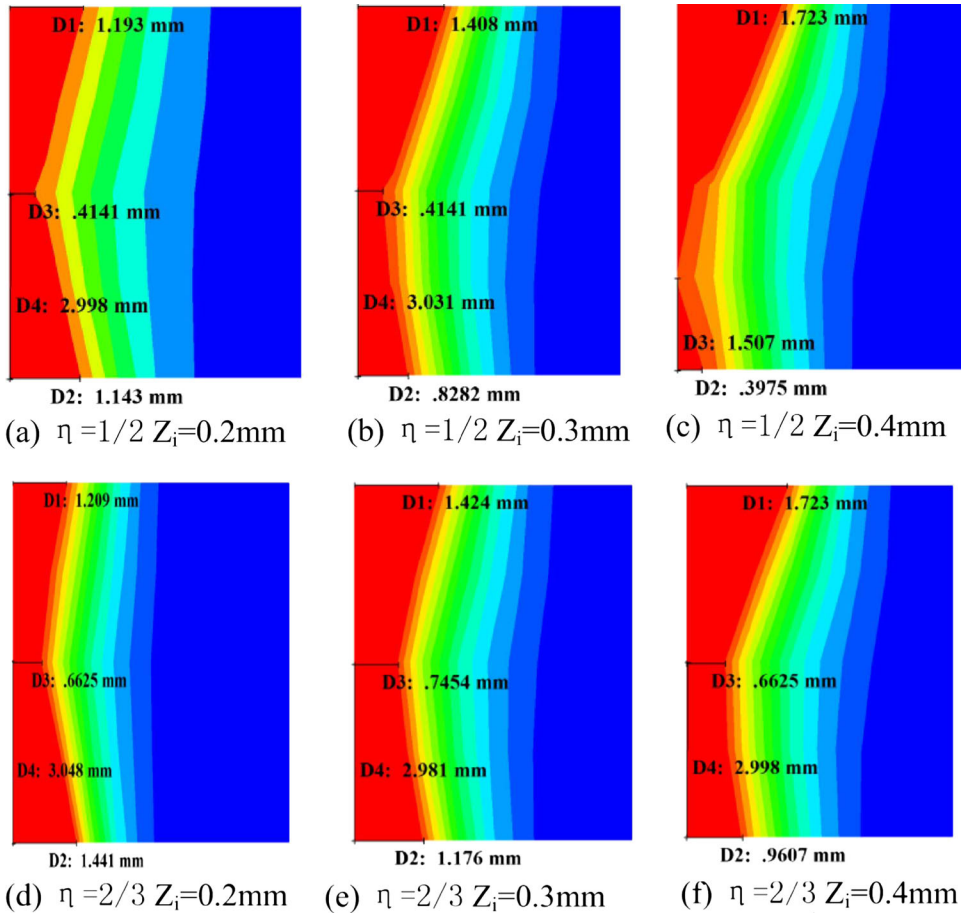

Fig. 8 The simulated cross section of welds (Power = 5000 W, Speed = 3 m/s)

The AverERRs for different welding parameter group are listed in Table 5.

The three best heat source parameters groups (combination of η and Z_i) are highlighted in red. According to Table 5, it is thought to be suitable to set Z_i to 3 mm, regardless of the values of laser beam power and welding speed. However, a smaller η is more appropriate when the weld speed increases. It is clear that the larger welding speed increases the attenuation of heat source intensity along z-axis direction. The virtual power for the bottom half of hourglass-like heat source should be reduced according to this trend. The comparison between the simulated temperature distribution on the cross section of weld and the physical weld for these three heat source parameters are shown in Fig. 13.

The predicted welding pool in Fig. 13a and b are very similar to the experimental welds, but in Fig. 13c the difference between simulated and experimental weld pool becomes larger. It can also be verified by Table 5. The AverERR for the 5000 w and 3.0 m/s parameters group is about 35 %, which is too large for an accuracy simulation. There are a lot of factors that can cause such large AverERR. The inappropriate choice for Z_e, Z_b, r_e, r_i, and r_b (the rest of heat source parameters which are set to constant before simulation) and too large Z_i may be the two main points. As mentioned above, the value of Z_e, Z_b, r_e, r_i, and r_b are determined based on the previous research for the conical heat source. Thus, more detail works need to be done to study the influence of these parameters on the shape of weld pool in the future. In addition, decreasing Z_i does not seem to be a good idea. A failure test by the authors

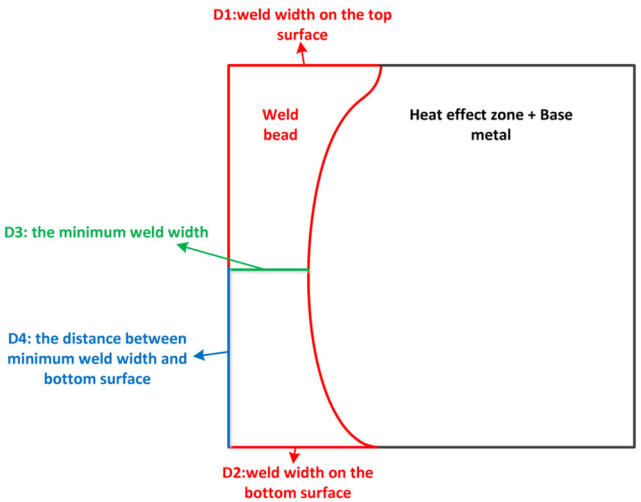

Fig. 9 The definition of D1–D4

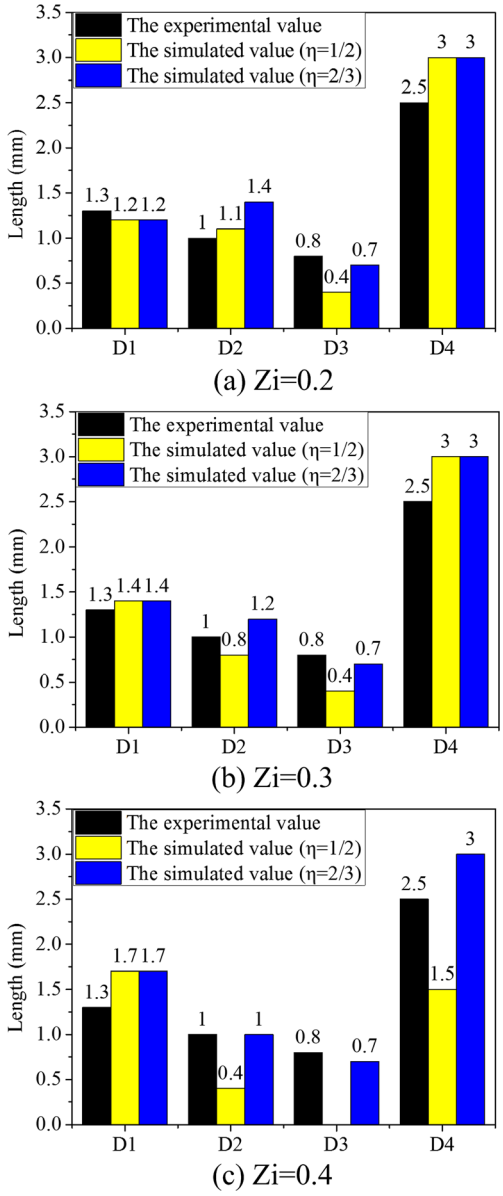

Fig. 10 The experimental and simulated values of D1–D4 (Power = 4000 W, Speed = 2.0 m/s)

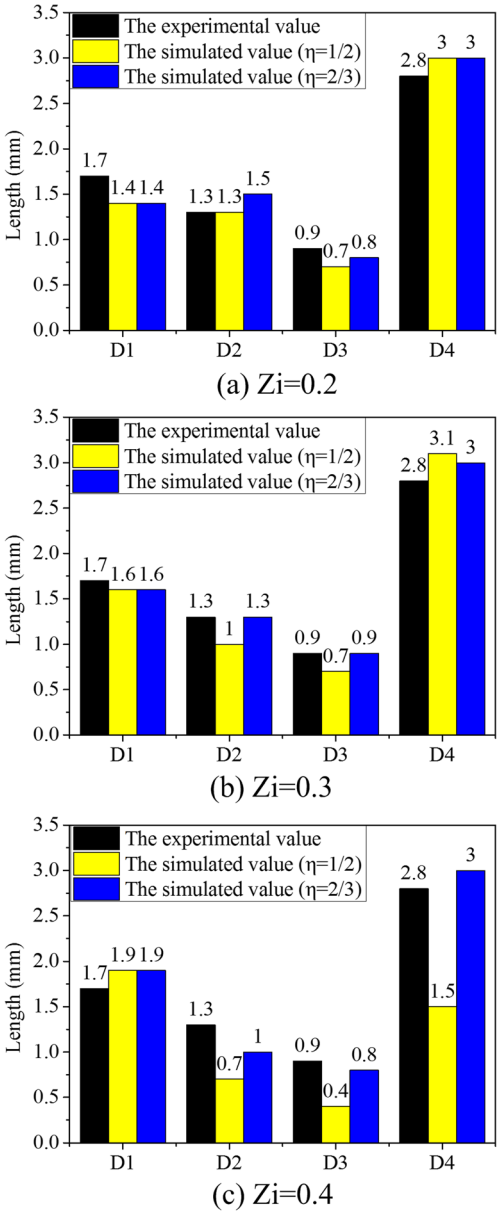

Fig. 11 The experimental and simulated values of D1–D4 (Power = 5000 W, Speed = 2.0 m/s)

illustrates that if Z_i equals to 1.5, the peak temperature will appear in the bottom of weld pool which is impossible during welding process.

5 Conclusions

An hourglass-like heat source model is developed in this work to give a more accurate prediction of laser beam welding for 1060 steel. Several conclusions can be achieved after a simulated and experimental investigation.

(1) The fully penetrated joint without porosities were obtained of laser welding for 6 mm thickness 1060 steel under three weld parameter groups: $P = 4000$ W, $S = 2$ m/min; $P = 5000$ W, $S = 2$ m/min; and $P = 5000$ W, $S = 3$ m/min.

(2) An hourglass heat source model was developed to represent the special appearance of the cross section after laser welding for 6 mm (middle thick) 1060 plates. The optimization of heat source parameters was carried out according to the error analysis. The heat source partition coefficient η equals to 2/3 and the z-axis coordinate of middle surface Zi equals to 0.3 is the best heat source parameter group for the welds with $P = 4000$ w and $S = 2$ m/min and $P = 5000$ w and $S = 2$ m/min as well as the heat source partition coefficient

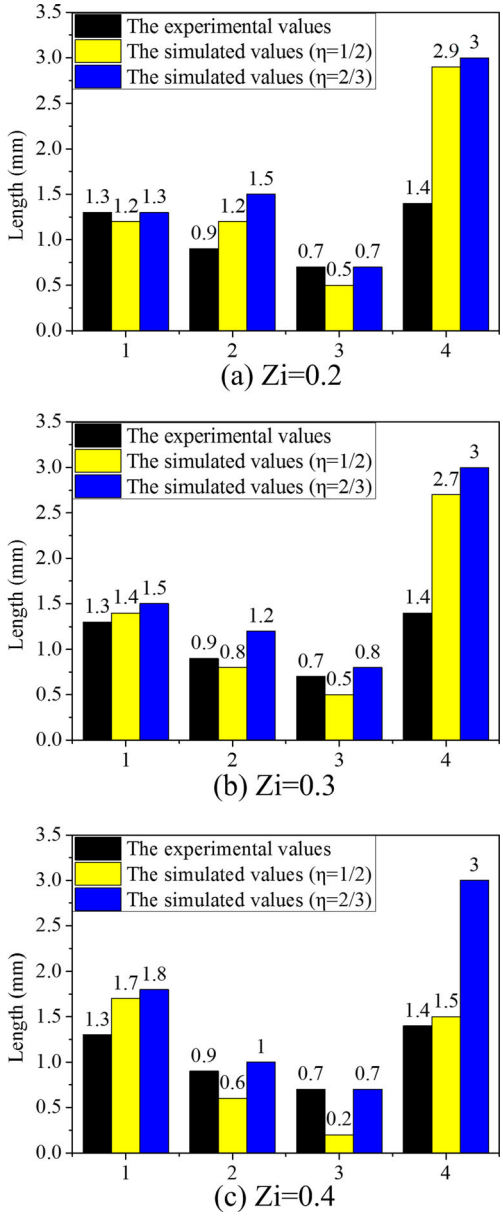

Fig. 12 The experimental and simulated values of D1–D4 (Power = 5000 W, Speed = 3.0 m/s)

Table 5 The values of AverERR for different welding parameters

	$P=4000$ W $S=2.0$ m/s	$P=5000$ W $S=2.0$ m/s	$P=5000$ W $S=3.0$ m/s
$\eta=2/3$, $Z_i=2$	0.2005	0.1282	0.4524
$\eta=2/3$, $Z_i=3$	0.1505	0.0326	0.4432
$\eta=2/3$, $Z_i=4$	0.1582	0.1327	0.4096
$\eta=1/2$, $Z_i=2$	0.2192	0.1175	0.4419
$\eta=1/2$, $Z_i=3$	0.2442	0.1547	0.3506
$\eta=1/2$, $Z_i=4$	0.5759	0.3998	0.3567

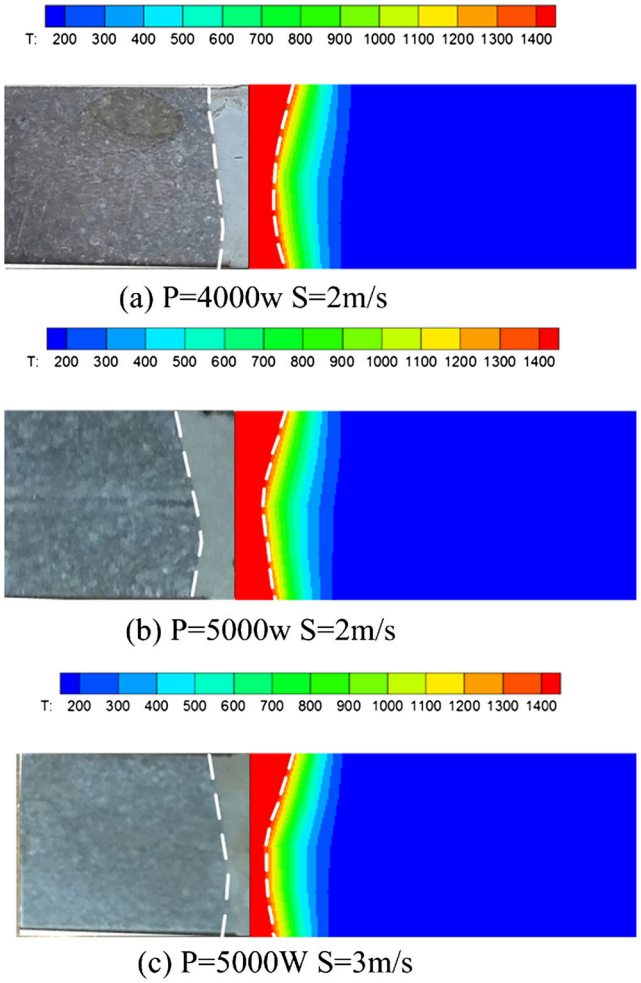

Fig. 13 The comparison between experimental and simulated welding cross section for different welding parameters

equals to 1/2 and the z-axis coordinate of middle surface equals to 0.3 is the best heat source parameters group for the welds with $P=5000$ W and $S=3$ m/min.

(3) According to the experimental and simulated investigation, it can be concluded that the width of weld has higher sensitivity on weld speed than laser power. To compare with experimental cross section, the hourglass-like heat source model is suitable to represent the geometry of laser beam penetration welds for 1060 steel because it brought a wider bottom weld width which is consisted with the actual shape.

Acknowledgments The authors gratefully acknowledge a Project Funded by the Priority Academic Program Development of Jiangsu Higher Education Institutions (PAPD) and the financial support of the project from the Fundamental Research Funds for the Central Universities (Grant No. NS2015058).

References

1. Cam G, Erim S, Yeni Ç, Koçak M (1999) Determination of mechanical and fracture properties of laser beam welded steel joints. Weld J 78(6):193–201
2. Çam G, Yeni Ç, Erim S, Ventzke V, Koçak M (1998) Investigation into properties of laser welded similar and dissimilar steel joints. Sci Technol Weld Join 3(4):177–189. doi:10.1179/stw.1998.3.4.177
3. Çam G, Koçak M (1998) Progress in joining of advanced materials. Int Mater Rev 43(1):1–44. doi:10.1179/imr.1998.43.1.1
4. Çam G, Koçak M (1998) Progress in joining of advanced materials: part 1: solid state joining, fusion joining, and joining of intermetallics. Sci Technol Weld Join 3(3):105–126. doi:10.1179/stw.1998.3.3.105
5. Lankalapalli K, Tuy J, Gartner M (1996) A model for estimating penetration depth of laser welding processes. J Phys D Appl Phys 29:1831–1841
6. Goldak J, Charkravariti A, Bibby M (1984) A new finite element model for welding heat sources. Metall Trans B 15B:299–305
7. Du H, Hu L, Liu J, Hu X (2004) A study on the metal flow in full penetration laser beam welding for titanium alloy. Comput Mater Sci 29(4):419–427. doi:10.1016/j.commatsci.2003.11.002
8. Buvanashekaran G, Siva Shanmugam N, Sankaranarayanasamy K, Sabarikanth R (2009) A study of laser welding modes with varying beam energy levels. Proc Inst Mech Eng C J Mech Eng Sci 223(5):1141–1156. doi:10.1243/09544062jmes1177
9. Li Y, Feng Y-H, Zhang X-X, Wu C-S (2013) An improved simulation of heat transfer and fluid flow in plasma arc welding with modified heat source model. Int J Therm Sci 64:93–104. doi:10.1016/j.ijthermalsci.2012.08.007
10. Sudnik W, Radaj D, Breitschwerdt S, Erofeew W (2000) Numerical simulation of weld pool geometry in laser beam welding. J Phys D Appl Phys 33:662–671
11. Dal M, Fabbro R (2016) [INVITED] An overview of the state of art in laser welding simulation. Opt Laser Technol 78:2–14. doi:10.1016/j.optlastec.2015.09.015
12. Hozoorbakhsh A, Ismail MIS, Aziz NBA (2015) A computational analysis of heat transfer and fluid flow in high-speed scanning of laser micro-welding. Int Commun Heat Mass Tran 68:178–187. doi:10.1016/j.icheatmasstransfer.2015.08.013
13. Garcia Navas V, Leunda J, Lambarri J, Sanz C (2015) Optimization of laser keyhole welding strategies of dissimilar metals by FEM simulation. Metall Mater Trans A 46(7):3140–3156. doi:10.1007/s11661-015-2906-4
14. Turner RP, Villa M, Sovani Y, Panwisawas C, Perumal B, Ward RM, Brooks JW, Basoalto HC (2015) An improved method of capturing the surface boundary of a Ti-6Al-4V fusion weld bead for finite element modeling. Metall Mater Trans B 47(1):485–494. doi:10.1007/s11663-015-0489-5
15. Karadeniz E, Ozsarac U, Yildiz C (2007) The effect of process parameters on penetration in gas metal arc welding processes. Mater Des 28(2):649–656. doi:10.1016/j.matdes.2005.07.014
16. Francis JA, Mazur W, Bhadeshia HKDH (2006) Type IV cracking in ferritic power plant steels. Mater Sci Technol 12:1387–1395
17. Goldak J, Akhlaghi M (2005) Computational welding mechanics. Springer US, New York
18. Mi G, Zhan X, Wei Y, Ou W, Gu C, Yu F (2015) A thermal–metallurgical model of laser beam welding simulation for carbon steels. Model Simul Mater Sci Eng 23(3):035010. doi:10.1088/0965-0393/23/3/035010